Characterisation of Antibody Interactions with the G Protein of Vesicular Stomatitis Virus Indiana Strain and Other Vesiculovirus G Proteins

Altar M Munis[a,b], Maha Tijani[a,b], Mark Hassall[c], Giada Mattiuzzo[c], Mary K Collins[a,b,d] and Yasuhiro Takeuchi[a,b]#.

[a]Division of Advanced Therapies, National Institute for Biological Standards and Control, South Mimms, UK

[b]Division of Infection and Immunity, University College London, London, UK

[c]Division of Virology, National Institute for Biological Standards and Control, South Mimms, UK

[d]Okinawa Institute of Science and Technology, Okinawa, Japan

Running Title: Interactions between antibodies and vesiculoviruses

#Correspondence should be addressed to Y.T.

Division of Infection and Immunity
Rm 228B The Rayne Building
5 University Street
University College London
WC1E 6JF
Tel: +44 20 3108 2144 (ext 52144).
Fax: +44 20 3108 2123
(y.takeuchi@ucl.ac.uk)

ABSTRACT

Vesicular stomatitis virus Indiana strain G protein (VSVind.G) is the most commonly used envelope glycoprotein to pseudotype lentiviral vectors (LV) for experimental and clinical applications. Recently, G proteins derived from other vesiculoviruses (VesG), for example Cocal virus, have been proposed as alternative LV envelopes with possible advantages compared to VSVind.G. Well-characterised antibodies that recognise VesG will be useful for vesiculovirus research, development of G protein-containing advanced therapy medicinal products (ATMPs), and deployment of VSVind-based vaccine vectors. Here we show that one commercially available monoclonal antibody, 8G5F11, binds to and neutralises G proteins from three strains of VSV as well as Cocal, and Maraba viruses, whereas the other commercially available monoclonal anti-VSVind.G antibody, IE9F9, binds to and neutralises only VSVind.G. Using a combination of G protein chimeras and site-directed mutations, we mapped the binding epitopes of IE9F9 and 8G5F11 on VSVind.G. IE9F9 binds close to the receptor binding site and competes with soluble low-density lipoprotein receptor (LDLR) for binding to VSVind.G, explaining its mechanism of neutralisation. In contrast, 8G5F11 binds close to a region known to undergo conformational changes when the G protein moves to its post-fusion structure, and we propose that 8G5F11 cross-neutralises VesGs by inhibiting this.

IMPORTANCE

VSVind.G is currently regarded as the gold-standard envelope to pseudotype lentiviral vectors. However, recently other G proteins derived from vesiculoviruses have been proposed as alternative envelopes. Here, we investigated two commercially available anti-VSVind.G monoclonal antibodies for their ability to cross-

react with other vesiculovirus G proteins, and identified the epitopes they recognise, and explored their neutralisation activity. We have identified 8G5F11, for the first time, as a cross-neutralising antibody against several vesiculovirus G proteins. Furthermore, we elucidated the two different neutralisation mechanisms employed by these two monoclonal antibodies. Understanding how cross-neutralising antibodies interact with other G proteins may be of interest in the context of host-pathogen interaction and co-evolution as well as providing the opportunity to modify the G proteins and improve G protein-containing medicinal products and vaccine vectors.

INTRODUCTION

The rhabdovirus, vesicular stomatitis virus Indiana stain (VSVind), has been used ubiquitously as a model system to study humoral and cellular immune responses in addition to being a promising virus for oncolytic virotherapy against cancer (1-3). Furthermore, its single envelope G protein (VSVind.G) is the most commonly used envelope to pseudotype lentiviral vectors and serves as the gold-standard in many experimental and clinical studies (4-6). Both receptor recognition and membrane fusion of the wild-type virus, as well as the pseudotyped particles, are mediated by this single transmembrane viral glycoprotein that homotrimerises and protrudes from the viral surface (7-9). Recently G proteins derived from other vesiculovirus subfamily members, namely, Cocal, Piry, and Chandipura viruses, have been proposed as alternative envelopes for lentiviral vector production due to some possible advantages over VSVind.G (10-12).

Although some antigenic and biochemical characteristics of VSVind.G have been reported (1, 7, 13-20), there is still little known about the other vesiculovirus G

proteins (VesG) and there is a general lack of reagents commercially available to identify, detect, and characterise them. In the past, monoclonal antibodies (mAbs) have been used to extensively study the antigenic determinants found on viral glycoproteins, e.g. hemagglutinin (HA) of influenza virus, the gp70 protein of murine leukaemia virus (MLV), and rabies virus G protein (21-25). These previous studies, especially on the influenza virus strains and the rabies virus have led to invaluable findings on the structure and function of the glycoproteins allowing identification of epitopes essential in virus neutralisation (25-27). In addition, mAbs have proven useful in viral pathogenesis studies as mutants selected by antibodies, in many cases demonstrated altered pathogenicity to their wild-type counterparts (28-30). Therefore, identification of antibodies that recognise VesG will not only be extremely valuable for vesiculovirus research but also aid in the development of G protein-containing advanced therapy medicinal products (ATMP) and vaccine vectors.

Here we show two anti-VSVind.G antibodies, 8G5F11 and a goat polyclonal antibody, VSV-Poly (31, 32), can cross-react with a variety of the VesG and cross-neutralise VesG-LV. We also demonstrate that the other commercially available extracellular monoclonal anti-VSVind.G antibody IE9F9 lacks this cross-reactivity. We further characterise the two mAbs, 8G5F11 and IE9F9, with regards to their relative affinities towards various VesG, binding epitopes, and cross-neutralisation strengths.

RESULTS

Investigation of antibody cross-reactivity with VesG

To investigate antibody binding to different vesiculovirus envelope glycoproteins (G proteins), we prepared plasmid pMD2-based vectors expressing six different

vesiculovirus G proteins (VesG): VSVind.G, Cocal virus G (COCV.G), Vesicular stomatitis virus New Jersey strain G (VSVnj.G), Piry virus G (PIRYV.G), Vesicular stomatitis virus Alagoas strain G (VSVala.G), and Maraba virus G (MARAV.G) (Figure 1A). HEK293T cells were transfected with these plasmid constructs, stained with the different antibodies, and analysed via flow cytometry. While IE9F9 only bound to VSVind.G, anti-VSVind.G monoclonal antibody 8G5F11 and VSV-Poly both could recognise various VesG with varying binding strengths (Figure 1B). PIRYV.G, the most distant vesiculovirus G investigated with approximately 40% identity to VSVind.G on amino acid level, could be recognised by VSV-Poly while 8G5F11 did not bind to it.

Characterisation of IE9F9 binding, 8G5F11 cross-reactivity and its affinity towards other VesG

To confirm that the difference of 8G5F11 binding to VesG was indicative of the mAb affinity towards VesG and not a difference in relative expression levels of the G proteins, we synthesised chimeric G proteins. The endogenous transmembrane and C-terminal domains of VesG were switched with that of VSVind.G (Figure 2A). Following the expression of these chimeric G proteins in HEK293T cells, we investigated 8G5F11 and IE9F9 binding saturation using quantitative flow cytometry while the relative expression levels of the G proteins were monitored using an intracellular anti-VSVind.G mAb, P5D4 (Figure 2B). 8G5F11 showed a wide range of affinities towards VesG: while its affinity for MARAV.G was comparable to that of VSVind.G, its interactions with COCV.G and VSVnj.G were much weaker.

To consolidate this finding, we further investigated these mAb-G protein interactions via surface plasmon resonance (SPR). First, to quantify mAb binding to G protein

120 monomers under conformationally correct folding, we immobilised wild-type (wt)
121 VSVind.G produced by thermolysin limited proteolysis of viral particles (Gth) (7, 17)
122 and tested the dose-dependent binding of the two mAbs (Figure 2C-D). The
123 measured Kd values for 8G5F11 and IE9F9 binding to VSVind.G were 2.76nM and
124 14.7nM respectively. To further analyse the VesG-8G5F11 interaction we
125 immobilised the mAb and investigated VesG pseudotyped lentiviral vector (LV)
126 binding. Since pseudotyped LV particles contain many trimeric G protein spikes
127 (33), the analysis of the interaction between VesG binding to immobilised 8G5F11
128 reflects avidity. A specific, vector dose-dependent binding (i.e. increasing binding
129 response with increasing titres) of VSVind.G was detected which saturated faster
130 than the mAb-Gth interaction. (Figure 2E). When identical doses of VesG-LV at
131 $1x10^8$ TU/ml were injected on immobilised 8G5F11, similar patterns of binding were
132 observed to that of quantitative flow cytometry, in the order of strength of VSVind >
133 MARAV > VSVala > Cocal > VSVnj (Figure 2F). Unrelated RDpro envelope
134 pseudotyped LVs were utilised as negative control to deduce unspecific interaction
135 of enveloped particles with immobilised mAb. PIRYV.G-LV demonstrated a similar
136 response to that of RDpro-LV indicative of the lack of binding between the G protein
137 and 8G5F11.

138 ***Determining the cross-neutralisation abilities of anti-VSVind.G antibodies***

139 These three antibodies were evaluated for their ability to neutralise VSVind.G and
140 VesG pseudotyped LVs (Figure 3). 8G5F11 demonstrated varying strengths of
141 neutralisation against VesG pseudotyped LVs, IC50 values ranging from 11.5ng/ml
142 to 86.9µg/ml (Figure 3A). There was however limited correlation between G
143 proteins' binding strength and sensitivity of LV, e.g. VSVnj.G-LV was more sensitive
144 than COCV.G-LV (Figure 3A) while COCV.G binding was stronger (Figure 1 and 2).

IE9F9 neutralised only VSVind.G-LV at 137ng/ml IC50, about 12-fold weaker than 8G5F11 (Figure 3B). In the case of VSV-Poly, we only observed cross neutralisation at high serum concentrations (Figure 3C). Furthermore, although VSV-Poly bound to PIRYV.G, it did not neutralise PIRYV.G-LVs.

Mapping the epitopes of anti-VSVind.G mAbs and identification of key amino acid residues that dictate antibody binding and neutralisation

To map where the neutralising antibodies might bind to on the G protein surface a series of chimeric G proteins between VSVind.G and COCV.G were constructed. The initial binding and neutralisation studies performed with these chimeras enabled us to narrow down the epitopes of these mAbs to lie between amino acid (aa) residues 137-369 on VSVind.G (data not shown). Furthermore, looking at previously published data on 8G5F11 and IE9F9's epitopes obtained through mutant virus escape assays (1, 13-15) we concentrated on two distinct regions on VSVind.G and synthesised 22 different mutant G proteins to study the epitopes (Figure 4). The mutants were cloned into the pMD2 backbone and their functionality were investigated via LV infection and antibody binding assays. All G proteins were confirmed to be functional and could successfully pseudotype LVs yielding comparable titres to their wild-type (wt) counterparts. Furthermore, their relative expression levels were monitored by intracellular P5D4 which also recognises the intracellular domain of COCV.G. Lastly, they could be detected by extracellular VSV-Poly implying there weren't any substantial protein display issues (data not shown).

We first investigated antibody binding to these G proteins via flow cytometry. Extracellular VSV-Poly and intracellular P5D4 stains determined relative expression

levels of the mutants. For both sets the relative difference between expression levels of mutant and wt proteins was in most cases less than two-fold (Figure 5A-B). In the case of 8G5F11, binding to VSVind.G mutants was reduced by approximately 100-fold while the changes on COCV.G enabled these mutants to bind to 8G5F11 at similar levels to that of wt VSVind.G (Figure 5C). This change in binding could also be observed on a western blot: while none of the VSVind.G mutants could be visualised, 8G5F11 could bind to COCV.G chimera C8.3 (data not shown). It can be inferred from these results that aa 257-259 (DKD) are the key residues that dictate 8G5F11 binding to G proteins.

On the other hand, for IE9F9 no statistically significant changes in antibody binding were observed for VSVind.G mutants (data not shown) except for chimeras V1.2 and V1.4 (Figure 5D). However, there was a substantial gain of binding effect for COCV.G mutants. While IE9F9 does not bind to wt COCV.G, mutations of amino acid residues LSR and AA (Figure 4) alone led to significant increase in the fluorescence signal, thus antibody binding, C1.4 with both LSR and AA had a comparable MFI level to that of wt VSVind.G.

Neutralisation profile of both VSVind.G and COCV.G mutants was also examined (Figure 5E-H). While LVs pseudotyped with VSVind.G mutants G, A, and N were not neutralised by 8G5F11 (Figure 5E), varying degrees of sensitivity were observed for COCV.G mutants with the strongest binder being the most sensitive (Figure 5F). On the other hand, this was not the case for IE9F9 mutants. While dose-dependent neutralisation of V1.2-LV was observed, VSVind.G mutant V1.4-LV was resistant to IE9F9 neutralisation (Figure 5G). Furthermore, no effect was observed on COCV.G mutant LV infection even though all bound to the mAb, some at similar levels to wt VSVind.G (Figure 5H). The data shows that while 8G5F11 employs a neutralisation

194 mechanism that is effective amongst the tested VesG, IE9F9's is VSVind.G specific
195 and binding does not necessarily result in neutralisation.

196 ***Investigation of neutralisation mechanisms utilised by the mAbs: binding***
197 ***competition with low-density lipoprotein receptor (LDLR)***

198 Antibodies neutralise viruses and viral vectors by several mechanisms. Many
199 neutralising antibodies (NAbs) prevent virions from interacting with cellular receptors
200 (34). VSVind.G's major receptor has been identified as the low-density lipoprotein
201 receptor (LDLR) (33, 35). Therefore, we investigated the binding competition
202 between 8G5F11 and IE9F9 with LDLR via SPR as a potential neutralisation
203 mechanism for the mAbs (Figure 6). Gth immobilised on the chip surface was
204 saturated with repeated injections of 8G5F11 and IE9F9. This was followed by an
205 injection of recombinant soluble human LDLR (sLDLR) and its binding to Gth was
206 examined. While sLDLR was able to bind to Gth following 8G5F11 saturation as well
207 as Gth without antibody exposure (buffer control), this interaction was almost
208 completely abrogated by IE9F9. These data suggest that IE9F9, but not 8G5F11,
209 neutralises VSVind.G-LV by blocking the G protein-receptor interaction either
210 through steric hindrance or direct competition.

211 ***8G5F11 blocks infection after endocytosis and before genome reverse***
212 ***transcription***

213 As demonstrated by the SPR data, 8G5F11 did not block receptor binding of the G
214 protein implying that it may be acting on LV infection steps following receptor
215 binding. Therefore, we investigated the internalisation of 8G5F11 bound LV particles
216 (Figure 7A). For this VSVind.G- and RDpro-LV, as well as unenveloped (env -ve)
217 LVs, were incubated with mAbs or plain OptiMEM and plated on HEK293T cells.

The level of LV which was internalised and therefore resistant to cell-trypsinisation was measured through reverse transcriptase (RT) activity 30min post-infection. RT activity measured in env -ve samples were regarded as unspecific uptake and regarded as background. RDpro-LVs, regardless of incubation with anti-VSVind.G mAbs, were internalised and so were VSVind.G-LVs in OptiMEM. While VSVind.G-LV incubated with IE9F9 demonstrated RT activity levels comparable to that of unenveloped LVs, 8G5F11 bound LV particles were endocytosed displaying RT activity similar to that of OptiMEM mixed VSVind.G-LV. In parallel infections total DNA was harvested 5h post-infection from VSVind.G-LV infected samples to determine reverse-transcribed provirus and transgene (GFP) copies via quantitative PCR and GFP expression was determined 48 post-infection via flow cytometry (Figure 7B). Reverse-transcribed LV copies and GFP expression were only detected in no mAb infections. Taken together, the data suggest that 8G5F11 blocks VSVind.G-LV infection following receptor binding and endocytosis of the vectors and before genome reverse transcription.

DISCUSSION

VSVind.G is the most commonly used envelope glycoprotein to pseudotype LVs for experimental and clinical applications. VSVind.G pseudotyped LVs can be produced in high titres and can infect a range of target cells. However, VSVind.G is cytotoxic to cells; thus, it is difficult to express it constitutively (36, 37). Moreover, VSVind.G pseudotyped LVs can be inactivated by human serum complement which limits their potential *in vivo* use (38-42). Therefore, there is a clear need for alternative envelopes to pseudotype LVs. Some of the most recent alternative envelopes that have been utilised are the G proteins of the other vesiculovirus family members (10-

12). However, one drawback of using these new G proteins is that there are no reagents commercially available to identify or characterise them.

In this study, we report that a commercially available anti-VSVind.G monoclonal antibody 8G5F11 can, unlike VSVind.G specific IE9F9, cross-react with a variety of the VesG and cross-neutralise VesG-LV. Furthermore, we explored the functional epitopes for both mAbs, identifying new amino acid substitutions in addition to previously reported ones (15), and elucidated their mechanism of neutralisation. G proteins of vesiculoviruses other than VSVind are being utilised for LV pseudotyping with the construction COCV.G-LV producer clones for *gfp* and T cell receptor-encoding LVs and the use of PIRYV.G and CHAV.G in transient LV production have been reported (10, 12, 43). We believe that the work presented will lay the groundwork for adaptation of VesG into new G-protein based advanced therapy medicinal products and allow for the utilisation of these commercially available antibodies in vesiculovirus and VesG-based gene therapy research.

The cross-reactive monoclonal 8G5F11 demonstrated interesting characteristics. Its high cross-reactivity even towards more distant relatives of VSVind.G such as VSVnj.G suggested that it might be recognising a well-conserved epitope. However, the results of the binding saturation assay didn't correlate with phylogenetic relativity. It revealed that its affinity towards COCV.G, one of the closest relatives of VSVind.G, was one of the weakest amongst the VesG investigated with almost a 250-fold difference compared to VSVind.G (Figure 2B).

This discrepancy can be explained through fine mapping of the 8G5F11 epitope. We identified the amino acids 257-259, DKD, as the key residues on VSVind.G for 8G5F11 binding. On VSVind.G the two negatively charged aspartic acid residues

266 flank the positively charged lysine possibly contributing towards the structure of the
267 α-helix form through salt-bridges (7, 16, 17). When either of the aspartic acid
268 residues is mutated to a neutral residue a significant reduction in binding is
269 observed. When this is compared to the corresponding three residues on other
270 VesG, the antibody binding is dependent on the overall charge of these three
271 residues rather than the ones surrounding them. In MARAV.G, these residues are
272 identical to VSVind.G, explaining why the antibody has similar strength of binding to
273 these two G proteins (Figure 8). On the other hand, VSVala.G binds 8G5F11 with
274 high affinity although these residues are not fully conserved, as in VSVala.G the
275 second aspartic acid residue is replaced with a glutamic acid. But it is possible that
276 the conservation of the second negative charge and the structural similarities
277 between these two residues enable a robust G protein-antibody interaction. Lastly,
278 the corresponding aa residues in PIRYV.G, VEQ, have electrostatically and
279 structurally different characteristics to that of lysine and aspartic acid leading to the
280 lack of interaction between the mAb and G protein.

281 We showed that IE9F9 recognises a β-sheet rich domain of the G protein (7, 17). A
282 complete abrogation of binding wasn't observed with the VSVind.G mutants
283 produced. This implies that the antibody either relies on other structural cues and
284 environmental charges around for binding or can utilise a secondary epitope.
285 However, through the gain of binding effect observed in COCV.G mutants, we were
286 able to identify two regions; AA and LSR, aa residues 352-353 and 356-358
287 respectively on VSVind.G, that are the key to this antibody's interaction.

288 All three reagents investigated demonstrated neutralising activities. 8G5F11 had the
289 greatest ability to cross-neutralise a wide array of vesiculovirus family members.
290 The strength of neutralisation for this mAb, however, didn't correlate with its affinity

291 towards other VesG (Figure 2 and 3). This suggests that innate differences, such as
292 protein structure, between the VesG might be playing a role in LV neutralisation.
293 Since the structures of the VesG other than VSVind.G and CHAV.G are not yet
294 delineated, it is hard to point out the key factors and mechanism involved accurately.
295 However, we have identified 8G5F11's epitope to lie close to the cross-over point
296 between pleckstrin homology and trimerisation domain of VSVind.G (7, 17, 19, 20,
297 35). Several hinge segments have been identified in the proximity of the epitope
298 which undergo large rearrangements in its relative orientation while the G protein
299 refolds from pre to post-fusion conformation in the low-pH conditions of the
300 endosomes following endocytosis (16, 19, 35). It can be hypothesised that 8G5F11
301 might be hindering this process ultimately preventing viral fusion and infection. As
302 pH-induced conformational changes during viral fusion is a shared characteristic
303 amongst VesG (44), this might be the underlying reason behind 8G5F11's ability to
304 cross-neutralise VesG-LV.

305 We have shown that IE9F9 blocks VSVind.G binding to its major receptor LDLR
306 (Figure 6). The crystal structures of VSVind.G in complex with LDLR domains have
307 been recently identified and have shown that VSVind.G can interact with two distinct
308 cysteine-rich domains (CR2 and CR3) of LDLR (35). One of the regions on
309 VSVind.G that is crucial for LDLR CR domain binding lies between amino acids 366-
310 370, only seven amino acids away from the key residues in IE9F9's epitope. The
311 key residues in this region of VSVind.G are not conserved amongst vesiculoviruses
312 therefore, neither the use of this epitope nor LDLR can be generalised to the other
313 members of the genus, making IE9F9's epitope and neutralisation mechanism
314 specific to VSVind.G. The lack of cross-reactivity and cross-neutralisation (Figure 1
315 and 3) displayed by the mAb towards VesG as well as its failure to neutralise

316 COCV.G mutants when its epitope is inserted into the G protein (Figure 5) suggest
317 specific requirement for binding mode between IE9G9 and G proteins to result in
318 neutralisation. Nikolic and colleagues have demonstrated that VSVind.G has
319 specifically evolved to interact with the CR domains of other LDLR family members
320 (35). The other members of the receptor family have already been identified as
321 secondary ports of entry for the virus (33). Complete neutralisation achieved with
322 IE9F9 indicates that the other LDLR family members might be interacting with the
323 same epitope on VSVind.G as well.

324 On the other hand, 8G5F11 does not interfere with receptor recognition (Figure 6)
325 and allows internalisation of the LV particles by the target cells (Figure 7A).
326 However, the vector genome does not get reverse transcribed and infection does not
327 occur implying 8G5F11 interferes with infection mechanisms after receptor binding
328 and internalisation of the particles. As discussed above 8G5F11's epitope is located
329 at the PH domain of the G protein in an α-helix around hinge regions that undergo
330 structural rearrangement. Our results, therefore, suggest that 8G5F11 may
331 neutralise VesG by interfering such conformational changes and membrane fusion.

332 Further work on these two identified epitopes regarding their immunodominance in
333 an *in vivo* setting and their detailed characterisation on other VesG from the
334 structure-function point of view may be of interest in the context of host-pathogen
335 interaction and co-evolution. This may also provide the opportunity for modifying
336 VSVind.G to improve G protein-containing advanced therapy medicinal products and
337 VSVind-based vaccine vectors.

338 **MATERIALS AND METHODS**

Cell culture. In all experiments, HEK293T cells were used. The cell line was maintained in Dulbecco's Modified Eagle Medium (DMEM) (Sigma-Aldrich, St Louis, MO) supplemented with 10% heat-inactivated foetal calf serum (Gibco, Carlsbad, CA), 2mM L-Glutamine (Gibco), 50 units/ml Penicillin (Gibco), 50µg/ml Streptomycin (Gibco). All cells were kept in cell culture incubators at 37ºC and 5% CO_2.

Phylogenetic analysis of vesiculovirus and rabies virus G proteins based on amino acid sequences. G proteins of the major vesiculoviruses (VSVind, UniProt Accession Number: P03522, Cocal virus, O56677, VSVnj, P04882, Piry virus, Q85213, Maraba virus, F8SPF4, VSVala, B3FRL4, Chandipura virus, P13180, Carajas virus, A0A0D3R1Y6, Isfahan virus, Q5K2K4) as well as the G protein of the Rabies virus (Q8JXF6), were included in the analysis. The amino acid sequences were aligned using ClustalOmega online multiple sequence alignment tool (EMBL-EPI). The evolutionary analyses were conducted in MEGA7 (45). The evolutionary history was inferred by using the maximum likelihood method based on the Jones-Taylor-Thornton matrix-based model (46). The tree with the highest likelihood is shown with the bootstrap confidence values (out of 100) indicated at the nodes. The tree is drawn to scale, with branch lengths measured in the number of substitutions per site, depicted in the linear scale. It should be noted that the amino acid sequence of the full-length G proteins (including the signal peptide) were referred to in this manuscript. Accordingly, reference to specific residue numbers is made in the context of these full-length sequences.

Plasmids used in experiments. VSVind.G expression plasmids, pMD2.G, and gag-pol expression plasmid p8.91 (47) were purchased from Plasmid Factory (Germany). GFP expressing self-inactivating vector plasmid used in the production of lentiviral vectors was produced in our lab previously (48, 49). pMD2.Cocal.G, COCV.G,

364 expression plasmid was a kindly provided by Hans-Peter Kiem (Fred Hutchinson
365 Cancer Research Center, Seattle, WA) . All other VesG envelopes were cloned into
366 this backbone using the restriction enzymes PmlI and EcoRI. Amino acid sequences
367 for VSVnj.G, PIRYV.G, MARAV.G, VSVala.G were retrieved from UniProt. Codon-
368 optimised genes were ordered from Genewiz (South Plainfield, NJ). Unrelated feline
369 endogenous virus RD114 derived RDpro envelope (49) was used as a negative
370 control.

371 **Gene transfer to mammalian cells.** Single plasmid transfection was used to
372 express VesG on HEK293T cell surface. HEK293T cells were seeded on the day
373 prior to transfection at $4x10^6$ cell per 10cm plate. These cells were transfected by
374 lipofection using FuGENE6 (Promega, Madison, WI) according to the manufacturer's
375 instructions. The cells were harvested 48h later to be used in various flow cytometry
376 assays.

377 **Overlapping extension PCR to synthesise VesG chimeras.** Phusion High-
378 Fidelity PCR Kit (NEB, Ipswich, MA) was used to perform the PCR reactions. All
379 primers used were obtained from Sigma-Aldrich. To splice two DNA molecules,
380 special primers were at the joining ends. For each molecule, the first of two PCRs
381 created a linear insert with a 5' overhang complementary to the 3' end of the
382 sequence from the other gene. Following annealing, these extensions allowed the
383 strands of the PCR product to act as a pair of oversized primers and the two
384 sequences were fused. Once both DNA molecules were extended, a second PCR
385 was carried out with only the flanking primers to amplify the newly created double-
386 stranded DNA of the chimeric gene.

Surface plasmon resonance. Analyses were performed using a BIAcore T100 instrument (GE Healthcare). Gth (0.04 mg/mL) and 8G5F11 (0.03 mg/mL) in sodium acetate buffers (10mM, pH 4.5 and 4.0 respectively) were immobilised on a CM5 sensor chip using the amine coupling system according to the manufacturer's instructions. To measure mAb affinity to VSVind.G, 8G5F11 (MW 155kDa) and IE9F9 (MW 155kDa) were suspended in HBS-EP (0.01M HEPES pH7.4, 0.15M NaCl, 3mM EDTA, 0.005v/v P20) and passed over the immobilised Gth at the indicated concentrations. To measure VesG-LV avidity against 8G5F11, LV preparations were suspended in HBS-EP buffer and passed over the immobilised mAb at indicated titers. The dissociation constants were calculated using BIAevaluation software according to the manufacturer's instructions. For the competitive binding assay, multiple injections of mAbs at 10µg/mL concentration was performed followed by injection of soluble recombinant LDLR (R&D Systems, Minneapolis, MN) at an identical concentration.

Use of molecules of equivalent soluble fluorochrome (MESF) system for quantitative flow-cytometry analysis. Quantum Alexa Fluor 647 MESF kit (Bangs Laboratories, Fishers, IN) was utilised for all quantitative fluorescence flow cytometry experiments. This is a microsphere kit that enables the standardisation of fluorescence intensity units. Beads with a pre-determined number of fluorophores are run on the same day and at the same fluorescence settings as stained cell samples to establish a calibration curve that relates the instrument channel values (i.e. median fluorescence intensity (MFI)) to standardised fluorescence intensity (MESF) units.

Extracellular and intracellular antibody binding assay. HEK293T cells were transfected to express the G proteins. 48 hours later cells were harvested, washed

412 twice with PBS and plated in U-bottom 96-well plates at identical densities. For
413 intracellular antibody binding assays cells were fixed with 1% formaldehyde (Sigma-
414 Aldrich, St Louis, MO) in PBS, permeabilised using 0.05% saponin (Sigma-Aldrich,
415 St Louis MO) in PBS and blocked with 1% bovine serum albumin (BSA, Sigma-
416 Aldrich, St Louis MO) in PBS. Cells were then incubated with serial dilutions of
417 extracellular and intracellular antibodies ranging from 0.1mg/ml to 2x10-7 mg/ml in
418 1% BSA (Sigma) in PBS in a total reaction volume of 200µl. After washing twice,
419 each sample was incubated with its respective fluorophore-conjugated secondary
420 antibody. Cells were then washed twice and resuspended in PBS. Stained cell
421 samples were analysed via flow cytometry using a FACSCanto II (BD Biosciences,
422 San Jose, CA) and Flowjo software. Primary antibodies used are as follows:
423 8G5F11 (I1 in (14)) and IE9F9 (I14 in (14)) (Kerafast, Boston, MA), VSV-Poly, a kind
424 gift from Prof Hiroo Hoshino and Dr Atsushi Oue (31, 32), P5D4 (Sigma-Aldrich).
425 Secondary antibodies used are as follows: Alexa Fluor® 647 conjugated anti-mouse
426 and anti-goat IgG (cat # 115-605-164 and 305-605-046 respectively, Jackson
427 Immunoresearch, UK).

428 **Transient LV production and concentration.** Three-plasmid co-transfection into
429 HEK293T cells was used to make pseudotyped LV as described previously (47).
430 Briefly, $4x10^6$ 293T cells were seeded in 10cm plates. 24 hours later, they were
431 transfected using FuGene6 (Promega, Madison, WI) with following plasmids: SIN
432 pHV (GFP expressing vector plasmid (48, 49)), p8.91 (Gag-Pol expression plasmid
433 (47)), and envelope expression plasmids. The medium was changed after 24 hours
434 and then vector containing media (VCM) was collected over 24-hour periods for 2
435 days. Following collection, VCM was passed through Whatman Puradisc 0.45µm
436 filters (SLS) and concentrated ~100-fold by ultra-centrifugation at 22,000 rpm

(87,119xg) for 2 hours at 4ºC in Beckmann Optima LK-90 ultracentrifuge using the SW-28 swinging bucket rotor (radius 16.1cm). The virus was resuspended in cold plain Opti-MEM on ice, aliquoted and stored at -80ºC.

LV titration. The functional titre of each vector preparation was determined by flow cytometric analysis for GFP expression following transduction of HEK293T cells. Briefly, $2x10^5$/well 293T cells were infected with LV plus 8 µg/ml polybrene (Merck-Millipore, Billerica, MA) for 24 hours. Infected cells were detected by GFP expression at 48 hours following the start of transduction. Titres were calculated from virus dilutions where 1–20% of the cell population was GFP-positive using the following formula:

$$\text{Titre}\left(\frac{\text{transduction units (TU)}}{\text{ml}}\right) = \frac{(\text{no. of cells at transduction}) \times (\%\text{ of GFP positive cells} \div 100) \times (\text{dilution factor})}{(\text{the volume of virus preparation added (ml)})}$$

Antibody neutralisation assay. To determine the neutralisation activity of anti-VSVind.G monoclonal and polyclonal antibodies an infection assay in the presence of antibodies was performed. Briefly, HEK293T cells were seeded in a 96-well plate at a density of $2x10^4$ cells/well with 200µl of medium containing 8µg/ml polybrene. Approximately 3 hours later, antibodies were serially diluted in plain Opti-MEM to 12 different concentrations/dilutions ranging from 0.5mg/ml (1:2 dilution) to $1.6x10^{-7}$ mg/ml (1:6,250,000 dilution). Each antibody dilution was mixed 1:1 with VesG-LV or mutant G-LV at $4.0x10^5$TU/ml titre to a final volume of 20µl, incubated at 37ºC for 1h and plated on the cells. 48 hours after cells were harvested and analysed for GFP expression by flow cytometry.

Site-directed mutagenesis PCR for production of mutant G proteins for epitope mapping. Site-directed mutagenesis (SMD) method was utilized to produce G protein mutants that were used in epitope mapping experiments. For this, QuikChange II XL Site-Directed Mutagenesis Kit (Agilent, Santa Clara, CA) was used. Initially, primers that would have the desired nucleotide changes were designed using the QuikChange Primer Design Tool (http://www.genomics.agilent.com/primerDesignProgram.jsp). All primers used were obtained from Sigma-Aldrich (St Louis, MO). The reaction was carried out according to manufacturer's instructions.

SYBR Green product-enhanced reverse transcriptase (SG-PERT)-based LV internalisation assay and quantitative PCR Assay. $2x10^4$ HEK293T cells/well were seeded in 24-well plates. $4.0x10^5$TU/ml titre of VSVind.G- and RDpro-LV as well as unenveloped LV (at a similar dilution) were mixed 1:1 v/v with plain OptiMEM or 0.1mg/ml of 8G5F11 or IE9F9 to a total volume of 20µl, incubated 1h at 37°C, and plated on cells. Following 30min incubation at 37°C samples for SG-PERT analysis (3 wells/condition) were harvested, washed and treated with trypsin-EDTA (0.25%) (Gibco) for 30min at 37°C. After, cells were lysed, and the SG-PERT was carried out as previously described (50, 51). In parallel, 5h post-incubation cells challenged with VSVind.G-LV were harvested (3 wells/condition) and total DNA was purified using the DNeasy Blood and Tissue Kit (Qiagen, Germany). 50ng of DNA was subjected to SYBR Green quantitative PCR using late RT (5'- CCCAACGAAGACAAGATCTGC-3' and 5'- TCCCATCGCGATCTAATTCTCC-3') and GFP (5'- CAACAGCCACAACGTCTATATCAT-3' and 5'- ATGTTGTGGCGGATCTTGAAG-3') primers to detect provirus as described previously (43). β-actin (5'- TGGACTTCGAGCAAGAGATG-3' and 5'-TTAAGTAGGCCGTCTTGCCT-3') was

used as the endogenous control. Infectivity was measured in parallel samples by flow cytometry 48h post infection.

Statistical Analyses. All statistical analyses were performed using GraphPad Prism 5 software (GraphPad, La Jolla, CA). Details of all tests, including the calculated p-values, are indicated in respective figure legends.

Funding

AMM and MT studentships are funded by NIBSC.

Acknowledgements

We would like to thank Prof Hiroo Hoshino and Dr Atsushi Oue (Gunma University, Japan), for providing us with a sample of the polyclonal goat anti-VSVind.G antibody, VSV-Poly and Drs Yves Gaudin and Aurélie Albertini for the Gth protein.

Author Contributions

A.M.M. performed experiments to obtain the presented data and wrote the paper. M.T. designed and produced the initial COCV.G/VSVind.G chimeras and obtained preliminary data on 8G5F11 binding to COCV.G-bearing cells. G.M. and M.H. helped in designing experiments and interpreting data. M.K.C. and Y.T. supervised the study, designed the experiments, interpreted the data, and wrote the paper.

Additional Information

Competing financial interest – Authors declare no competing financial interests.

REFERENCES

1. Keil W, Wagner RR. 1989. Epitope mapping by deletion mutants and chimeras of two vesicular stomatitis virus glycoprotein genes expressed by a vaccinia virus vector. Virology 170:392-407.
2. Wagner RR. 1987. Rhabdovirus biology and infection: An overview., p 9-74. *In* Wagner RR (ed), The Rhabdoviruses. Plenum, New York.
3. Hastie E, Grdzelishvili VZ. 2012. Vesicular stomatitis virus as a flexible platform for oncolytic virotherapy against cancer. Journal of General Virology 93:2529-2545.
4. Naldini L, Blomer U, Gallay P, Ory D, Mulligan R, Gage FH, Verma IM, Trono D. 1996. In vivo gene delivery and stable transduction of nondividing cells by a lentiviral vector. Science 272:263-267.
5. Bhella RS, Nichol ST, Wanas E, Ghosh HP. 1998. Structure, expression and phylogenetic analysis of the glycoprotein gene of Cocal virus. Virus Res 54:197-205.
6. Reiser J, Harmison G, KluepfelStahl S, Brady RO, Karlson S, Schubert M. 1996. Transduction of nondividing cells using pseudotyped defective high-titer HIV type 1 particles. Proceedings of the National Academy of Sciences of the United States of America 93:15266-15271.
7. Roche S, Rey FA, Gaudin Y, Brassanelli S. 2007. Structure of the pre-fusion form of the vesicular stomatitis virus glycoprotein g. Science 315:843-848.
8. Bishop DH, Repik P, Obijeski JF, Moore NF, Wagner RR. 1975. Restitution of infectivity to spikeless vesicular stomatitis virus by solubilized viral components. J Virol 16:75-84.
9. Matlin KS, Reggio H, Helenius A, Simons K. 1982. Pathway of vesicular stomatitis virus entry leading to infection. J Mol Biol 156:609-31.
10. Humbert O, Gisch DW, Wohlfahrt ME, Adams AB, Greenberg PD, Schmitt TM, Trobridge GD, Kiem HP. 2016. Development of Third-generation Cocal Envelope Producer Cell Lines for Robust Lentiviral Gene Transfer into Hematopoietic Stem Cells and T-cells. Mol Ther 24:1237-46.

528 11. Trobridge GD, Wu RA, Hansen M, Ironside C, Watts KL, Olsen P, Beard BC, Kiem HP. 2010.
529 Cocal-pseudotyped lentiviral vectors resist inactivation by human serum and efficiently
530 transduce primate hematopoietic repopulating cells. Mol Ther 18:725-33.
531 12. Hu S, Mohan Kumar D, Sax C, Schuler C, Akkina R. 2016. Pseudotyping of lentiviral vector
532 with novel vesiculovirus envelope glycoproteins derived from Chandipura and Piry viruses.
533 Virology 488:162-8.
534 13. Lefrancois L, Lyles DS. 1983. Antigenic determinants of vesicular stomatitis virus: analysis
535 with antigenic variants. J Immunol 130:394-8.
536 14. Lefrancois L, Lyles DS. 1982. The interaction of antibody with the major surface glycoprotein
537 of vesicular stomatitis virus. I. Analysis of neutralizing epitopes with monoclonal antibodies.
538 Virology 121:157-67.
539 15. Vandepol SB, Lefrancois L, Holland JJ. 1986. Sequences of the major antibody binding
540 epitopes of the Indiana serotype of vesicular stomatitis virus. Virology 148:312-25.
541 16. Roche S, Albertini AAV, Lepault J, Bressanelli S, Gaudin Y. 2008. Structures of vesicular
542 stomatitis virus glycoprotein: membrane fusion revisited. Cellular and Molecular Life
543 Sciences 65:1716-1728.
544 17. Roche S, Bressanelli S, Rey FA, Gaudin Y. 2006. Crystal structure of the low-pH form of the
545 vesicular stomatitis virus glycoprotein G. Science 313:187-91.
546 18. Albertini AA, Merigoux C, Libersou S, Madiona K, Bressanelli S, Roche S, Lepault J, Melki R,
547 Vachette P, Gaudin Y. 2012. Characterization of Monomeric Intermediates during VSV
548 Glycoprotein Structural Transition. Plos Pathogens 8.
549 19. Baquero E, Albertini AA, Raux H, Abou-Hamdan A, Boeri-Erba E, Ouldali M, Buonocore L,
550 Rose JK, Lepault J, Bressanelli S, Gaudin Y. 2017. Structural intermediates in the fusion-
551 associated transition of vesiculovirus glycoprotein. EMBO J 36:679-692.

552 20. Baquero E, Albertini AA, Vachette P, Lepault J, Bressanelli S, Gaudin Y. 2013. Intermediate
553 conformations during viral fusion glycoprotein structural transition. Current Opinion in
554 Virology 3:143-150.
555 21. Benmansour A, Leblois H, Coulon P, Tuffereau C, Gaudin Y, Flamand A, Lafay F. 1991.
556 Antigenicity of Rabies Virus Glycoprotein. Journal of Virology 65:4198-4203.
557 22. Lubeck MD, Gerhard W. 1981. Topological mapping antigenic sites on the influenza
558 A/PR/8/34 virus hemagglutinin using monoclonal antibodies. Virology 113:64-72.
559 23. Webster RG, Laver WG. 1980. Determination of the number of nonoverlapping antigenic
560 areas on Hong Kong (H3N2) influenza virus hemagglutinin with monoclonal antibodies and
561 the selection of variants with potential epidemiological significance. Virology 104:139-48.
562 24. Stone MR, Nowinski RC. 1980. Topological mapping of murine leukemia virus proteins by
563 competition-binding assays with monoclonal antibodies. Virology 100:370-81.
564 25. Seif I, Coulon P, Rollin PE, Flamand A. 1985. Rabies virulence: effect on pathogenicity and
565 sequence characterization of rabies virus mutations affecting antigenic site III of the
566 glycoprotein. J Virol 53:926-34.
567 26. Wiley DC, Wilson IA, Skehel JJ. 1981. Structural identification of the antibody-binding sites of
568 Hong Kong influenza haemagglutinin and their involvement in antigenic variation. Nature
569 289:373-8.
570 27. Hovanec DL, Air GM. 1984. Antigenic structure of the hemagglutinin of influenza virus
571 B/Hong Kong/8/73 as determined from gene sequence analysis of variants selected with
572 monoclonal antibodies. Virology 139:384-92.
573 28. Dietzschold B, Wunner WH, Wiktor TJ, Lopes AD, Lafon M, Smith CL, Koprowski H. 1983.
574 Characterization of an antigenic determinant of the glycoprotein that correlates with
575 pathogenicity of rabies virus. Proc Natl Acad Sci U S A 80:70-4.
576 29. Spriggs DR, Fields BN. 1982. Attenuated reovirus type 3 strains generated by selection of
577 haemagglutinin antigenic variants. Nature 297:68-70.

578 30. Zondag GCM, Postma FR, Van Etten I, Verlaan I, Moolenaar WH. 1998. Sphingosine 1-
579 phosphate signalling through the G-protein-coupled receptor Edg-1. Biochemical Journal
580 330:605-609.
581 31. Tamura K, Oue A, Tanaka A, Shimizu N, Takagi H, Kato N, Morikawa A, Hoshino H. 2005.
582 Efficient formation of vesicular stomatitis virus pseudotypes bearing the native forms of
583 hepatitis C virus envelope proteins detected after sonication. Microbes and Infection 7:29-
584 40.
585 32. Hoshino H, Nakamura T, Tanaka Y, Miyoshi I, Yanagihara R. 1993. Functional conservation of
586 the neutralizing domains on the external envelope glycoprotein of cosmopolitan and
587 melanesian strains of human T cell leukemia/lymphoma virus type I. J Infect Dis 168:1368-
588 73.
589 33. Finkelshtein D, Werman A, Novick D, Barak S, Rubinstein M. 2013. LDL receptor and its
590 family members serve as the cellular receptors for vesicular stomatitis virus. Proceedings of
591 the National Academy of Sciences of the United States of America 110:7306-7311.
592 34. Klasse PJ. 2014. Neutralization of Virus Infectivity by Antibodies: Old Problems in New
593 Perspectives. Adv Biol 2014.
594 35. Nikolic J, Belot L, Raux H, Legrand P, Gaudin Y, A AA. 2018. Structural basis for the
595 recognition of LDL-receptor family members by VSV glycoprotein. Nat Commun 9:1029.
596 36. Burns JC, Friedmann T, Driever W, Burrascano M, Yee JK. 1993. Vesicular stomatitis virus G
597 glycoprotein pseudotyped retroviral vectors: concentration to very high titer and efficient
598 gene transfer into mammalian and nonmammalian cells. Proc Natl Acad Sci U S A 90:8033-7.
599 37. Hoffmann M, Wu YJ, Gerber M, Berger-Rentsch M, Heimrich B, Schwemmle M, Zimmer G.
600 2010. Fusion-active glycoprotein G mediates the cytotoxicity of vesicular stomatitis virus M
601 mutants lacking host shut-off activity. J Gen Virol 91:2782-93.
602 38. Tesfay MZ, Ammayappan A, Federspiel MJ, Barber GN, Stojdl D, Peng KW, Russell SJ. 2014.
603 Vesiculovirus neutralization by natural IgM and complement. J Virol 88:6148-57.

604 39. Tesfay MZ, Kirk AC, Hadac EM, Griesmann GE, Federspiel MJ, Barber GN, Henry SM, Peng
605 KW, Russell SJ. 2013. PEGylation of Vesicular Stomatitis Virus Extends Virus Persistence in
606 Blood Circulation of Passively Immunized Mice. Journal of Virology 87:3752-3759.
607 40. Beebe DP, Cooper NR. 1981. Neutralization of Vesicular Stomatitis-Virus (Vsv) by Human-
608 Complement Requires a Natural Igm Antibody Present in Human-Serum. Journal of
609 Immunology 126:1562-1568.
610 41. DePolo NJ, Reed JD, Sheridan PL, Townsend K, Sauter SL, Jolly DJ, Dubensky TW, Jr. 2000.
611 VSV-G pseudotyped lentiviral vector particles produced in human cells are inactivated by
612 human serum. Mol Ther 2:218-22.
613 42. Croyle MA, Callahan SM, Auricchio A, Schumer G, Linse KD, Wilson JM, Brunner LJ, Kobinger
614 GP. 2004. PEGylation of a vesicular stomatitis virus G pseudotyped lentivirus vector prevents
615 inactivation in serum. Journal of Virology 78:912-921.
616 43. Tijani M, Munis AM, Perry C, Sanber K, Ferraresso M, Mukhopadhyay T, Themis M, Nisoli I,
617 Mattiuzzo G, Collins MK, Takeuchi Y. 2018. Lentivector producer cell lines with stably
618 expressed vesiculovirus envelopes. Molecular Therapy: Methods & Clinical Development
619 doi:10.1016/j.omtm.2018.07.013.
620 44. Baquero E, Albertini AA, Gaudin Y. 2015. Recent mechanistic and structural insights on class
621 III viral fusion glycoproteins. Curr Opin Struct Biol 33:52-60.
622 45. Kumar S, Stecher G, Tamura K. 2016. MEGA7: Molecular Evolutionary Genetics Analysis
623 Version 7.0 for Bigger Datasets. Mol Biol Evol 33:1870-4.
624 46. Jones DT, Taylor WR, Thornton JM. 1992. The rapid generation of mutation data matrices
625 from protein sequences. Comput Appl Biosci 8:275-82.
626 47. Zufferey R, Nagy D, Mandel RJ, Naldini L, Trono D. 1997. Multiply attenuated lentiviral vector
627 achieves efficient gene delivery in vivo. Nat Biotechnol 15:871-5.

628 48. Knight S, Sanber K, Stephen S, Ferraresso M, Baley R, Escors D, Santilli G, Thrasher A, Collins
629 M, Takeuchi Y. 2014. A clinical-grade constitutive packaging cell line for the production of
630 self-inactivating lentiviral vectors. Human Gene Therapy 25:A101-A102.
631 49. Sanber KS, Knight SB, Stephen SL, Bailey R, Escors D, Minshull J, Santilli G, Thrasher AJ,
632 Collins MK, Takeuchi Y. 2015. Construction of stable packaging cell lines for clinical lentiviral
633 vector production. Scientific Reports 5.
634 50. Pizzato M, Erlwein O, Bonsall D, Kaye S, Muir D, McClure MO. 2009. A one-step SYBR Green
635 I-based product-enhanced reverse transcriptase assay for the quantitation of retroviruses in
636 cell culture supernatants. J Virol Methods 156:1-7.
637 51. Vermeire J, Naessens E, Vanderstraeten H, Landi A, Iannucci V, Van Nuffel A, Taghon T,
638 Pizzato M, Verhasselt B. 2012. Quantification of reverse transcriptase activity by real-time
639 PCR as a fast and accurate method for titration of HIV, lenti- and retroviral vectors. PLoS One
640 7:e50859.
641 52. Waterhouse AM, Procter JB, Martin DMA, Clamp M, Barton GJ. 2009. Jalview Version 2-a
642 multiple sequence alignment editor and analysis workbench. Bioinformatics 25:1189-1191.

643

644 **FIGURE LEGENDS**

645 **Figure 1: 8G5F11 and VSV-Poly cross-react with a variety of VesG while IE9F9**
646 **only binds to VSVind.G.** **(A)** G proteins of the major vesiculoviruses, as well as the
647 G protein of the rabies virus (RABV), were analysed with regards to their
648 phylogenetic relationship. The tree amongst VesG is drawn to scale, with branch
649 lengths measured in the number of substitutions per site, depicted in the linear scale.
650 VSVind: Vesicular stomatitis virus Indiana strain, COCV: Cocal virus, VSVnj:
651 Vesicular stomatitis virus New Jersey strain, PIRYV: Piry virus, CJSV: Carajas virus,
652 CHAV: Chandipura virus, ISFV: Isfahan virus, MARAV: Maraba virus, VSVala:
653 Vesicular stomatitis virus Alagoas strain. Vesiculoviruses that we investigated are
654 highlighted in boxes and percentage amino acid identities to VSVind.G are
655 summarised in the table on the right-hand side. **(B)** Histograms represent the
656 binding of the antibodies to the VesG expressed on the surface of transfected
657 HEK293T cells. The strength of cross-reaction is depicted via the different MFIs of
658 the histograms. Data shown is one of the three repeats performed.

659 **Figure 2: Investigation of 8G5F11 and IE9F9 affinities towards VSVind.G and**
660 **characterisation of 8G5F11 cross-reactivity.** **(A)** Schematic representation of the
661 chimeric vesiculovirus G proteins with VSVind.G transmembrane and C-terminal
662 domains. **(B)** HEK293T cells expressing chimeric VesG were incubated with serial
663 dilutions of 8G5F11 and analysed via flow cytometry. MFIs of the fluorescent signals
664 were converted into the number of fluorophores using the MESF standard curve
665 according to manufacturer's instructions, the background signal from mock-
666 transfected HEK293Ts was subtracted and binding saturation curves were plotted.
667 The varying affinity of the mAb towards different VesG is demonstrated by the shift in
668 the slope of the binding curves. The curves were fitted, and dissociation constants

(Kd) calculated using the software GraphPad Prism 5 modelling the interaction as 1:1 specific binding: VSVind.G: $2.64x10^{-9}$M, COCV.G: $5.88x10^{-7}$M, VSVnj.G: $1.57x10^{-7}$M, MARAV.G: $4.13x10^{-9}$M, VSVala.G: $3.09x10^{-9}$M. Data shown represent the mean of three repeats performed in duplicates. **(inset)** The expression levels of the chimeric G proteins were determined via intracellular P5D4 staining. Data shown represent the mean +/- SD of three repeats performed in duplicates. Surface plasmon resonance (SPR) analysis of **(C)** 8G5F11 and **(D)** IE9F9 binding to immobilized Gth in HBS-EP buffer. **(E)** Surface plasmon resonance analysis of VSVind.G-LV binding to immobilised 8G5F11 in HBS-EP buffer. **(F)** Surface plasmon resonance analysis of Ves.G-LV ($1x10^{8}$ TU/ml) binding to immobilized 8G5F11 in HBS-EP buffer. The binding curves are normalised with regards to the relative response of unenveloped LV particles (Env -ve) which is regarded as the background. SPR data shown is one of the three repeats performed.

Figure 3: Neutralisation activity of mAbs and VSV-Poly. Neutralisation of VesG-LV by **(A)** 8G5F11, **(B)** IE9F9, and **(C)** VSV-Poly. Solid lines signify the neutralisation effect observed while the dotted lines indicate the lack of neutralisation. **(D)** Calculated IC50 values for 8G5F11 and IE9F9, depicting the potency of neutralisation. The curves were fitted using the software GraphPad Prism 5 modelled as an [inhibitor] vs. response curve with variable Hill Slopes and IC50 values calculated. Data shown represent the mean +/- SD of three repeats.

Figure 4: Mutants and chimeric G proteins produced for epitope mapping. Mutants and chimeras produced for epitope mapping of monoclonal antibodies **(A)** 8G5F11 and **(B)** IE9F9. Names and linear representations of the mutants and chimeras are listed on either side of the amino acid alignments of the regions where mutations were made. The boundaries are labelled with respective amino acid

numbers. Amino acid alignment legend: Black, residues from wt VSVind.G; white with black background, residues from wt COCV.G; grey, shared residues; blue, previously identified mutants (15); red, VSVind.G residues switched into COCV.G; green, COCV.G residues switched into VSVind.G. Linear G protein representations: the regions that the mutations were carried out at are represented by dotted lines. Black bars represent wt VSVind.G sequences while grey-bordered bars are for wt COCV.G residues. Point mutations are denoted by a bar and a circle.

Figure 5: Investigation of antibody binding to mutant G proteins and neutralisation of mutant-LVs. HEK293T cells were transfected to express the mutant G proteins on their surface. **(A-B)** The cells expressing chimeric mutants were stained with extracellular VSV-Poly (white bars) and intracellular P5D4 (grey bars) as expression control for the G proteins. The measured MFI values were normalised to the wt VesG signals for each set of mutants. The same population of cells were also incubated with **(C)** 8G5F11 and **(D)** IE9F9 at saturating concentrations. One-way ANOVA analysis with Dunnett's post-test was performed to compare the MFI values of mutant G proteins to that of their wild-type counterpart. Legged lines denote the significance of a single comparison, while straight lines signify all the individual comparisons within the group share the denoted significance unless otherwise stated (*, $p<0.05$; **, $p<0.01$; ***, $p<0.001$). This assay was performed three times in duplicates; mean +/- SD is plotted above. The neutralisation curves for select mutant and chimeric G pseudotyped LVs are plotted for **(E-F)** 8G5F11 and **(G-H)** IE9F9. Solid lines signify the neutralisation effect observed. **(E and G)** Previously reported reductions in binding for VSVind.G mutants translated into either complete or partial resistance to neutralisation by both antibodies. For COCV.G mutants **(F and H),** the mutations conferred the G proteins

sensitivity to neutralisation by 8G5F11 but not by IE9F9. The curves were fitted using the software GraphPad Prism 5 modelled as an [inhibitor] vs. response curve with variable Hill Slopes. Data shown represent the mean from three experiments performed in independent triplicates.

Figure 6: IE9F9 hinders sLDLR binding to Gth. 8G5F11 and IE9F9 were injected over immobilised Gth at 10µg/ml concentration three times to achieve binding saturation. Following this, sLDLR was injected over the chip at a concentration of 10µg/ml and its binding to Gth was measured. As buffer control an identical sLDLR injection was performed following multiple injections of HBS-EP running buffer. Measured sLDLR binding levels are indicated above the binding response curves and times of injections are marked with arrows. The data presented represent one of the three repeats performed.

Figure 7: Internalisation but not reverse transcription of 8G5F11 bound LVs. **(A)** VSVind.G- and RDpro-LVs as well as env -ve LVs were incubated with plain OptiMEM or 8G5F11 or IE9F9 and plated on HEK293T cells. After allowing internalisation of the particles cells were lysed and RT activity measured via SG-PERT. The black bars represent the initial viral inputs plated on cells. The data shown represent mean +/- SEM of two repeats performed in triplicates. **(B)** In parallel infections total DNA was extracted 5h post-infection and reverse-transcribed provirus and transgene copies were quantified via qPCR and normalised to β-actin copies. The data shown represent mean +/- SEM of an experiment performed in independent triplicates. GFP expression was determined 48h post-infection via flow cytometry. Each point represents an independent triplicate and the line stands for the median.

743 **Figure 8: Comparison of 8G5F11's epitope in other VesG through amino acid**
744 **alignment.** Amino acid residues for the vesiculovirus G proteins were retrieved from
745 UniProt. The sequences were aligned using ClustalOmega online multiple sequence
746 alignment tool (EMBL-EPI), and the alignments were visualised using JalView
747 software (52). The boundaries are labelled with respective amino acid numbers.
748 Dashed lines represent gaps introduced to maximise matching of amino acid
749 residues. Blue shading indicates percent identity; dark blue: 80-100%, medium blue:
750 60-80% light blue: 40-60%, and no colour indicating <40% identity. Amino acid
751 residues that dictate 8G5F11 binding are highlighted in a red box.

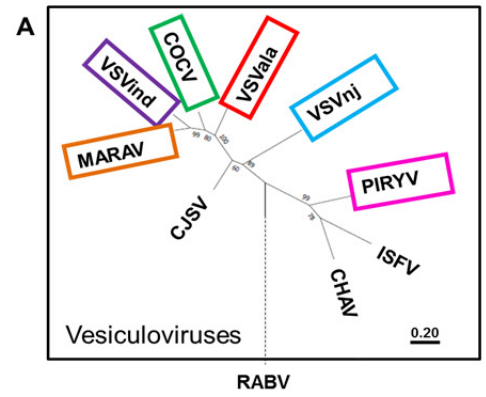

Virus	%Amino acid identity to VSVind.G
VSVindiana	100%
Maraba	78%
Cocal	72%
VSValagoas	64%
VSVnew jersey	50%
Piry	40%

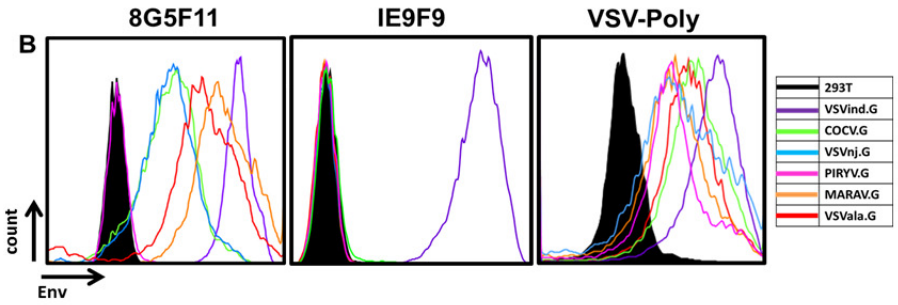

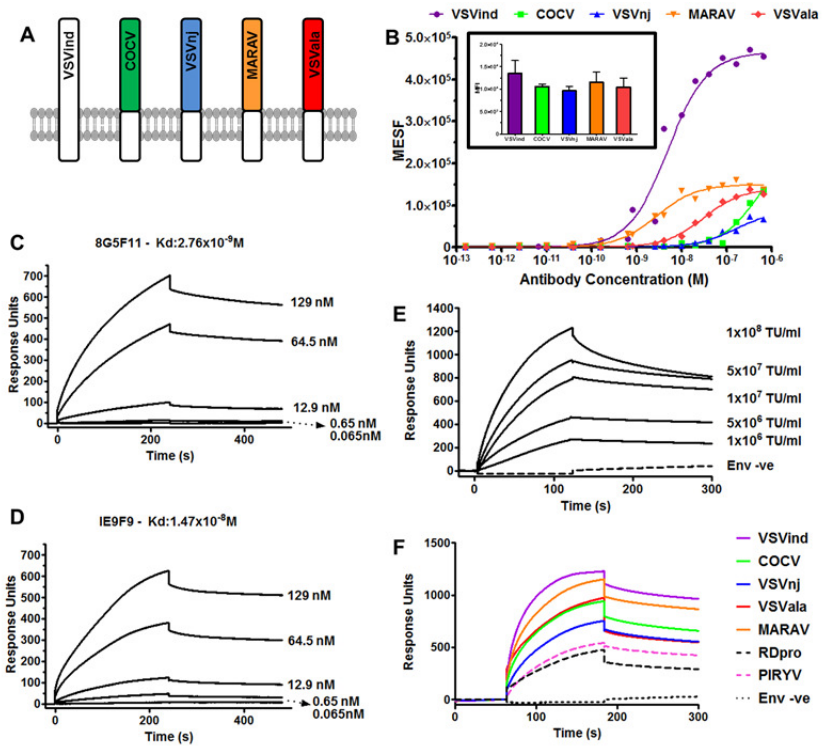

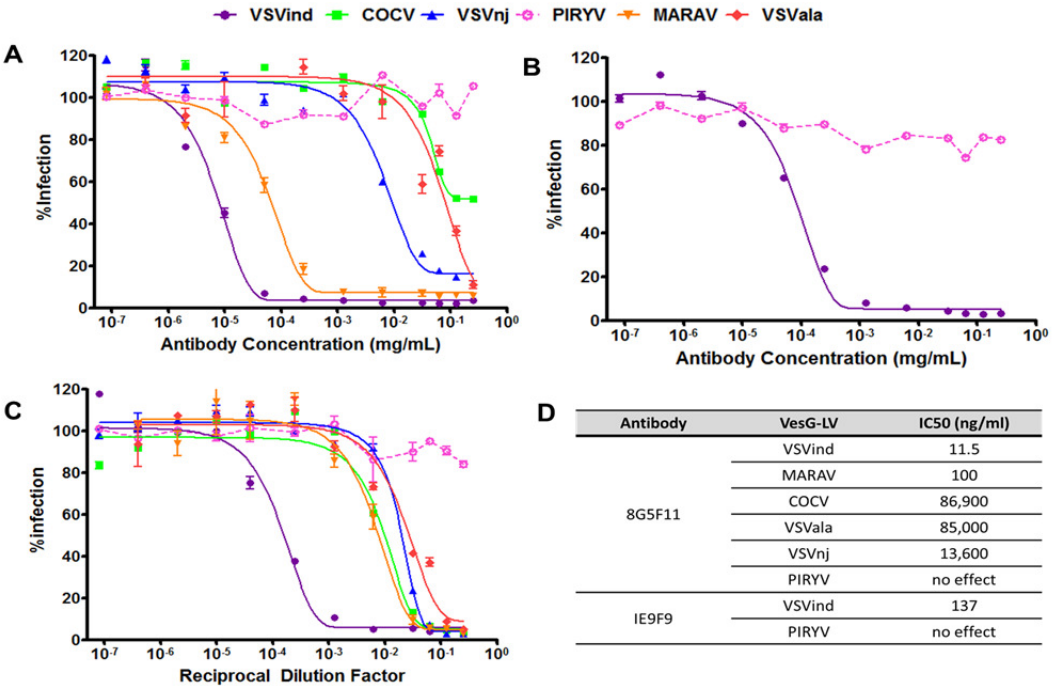

D

Antibody	VesG-LV	IC50 (ng/ml)
8G5F11	VSVind	11.5
	MARAV	100
	COCV	86,900
	VSVala	85,000
	VSVnj	13,600
	PIRYV	no effect
IE9F9	VSVind	137
	PIRYV	no effect